



## مدولاسیون نوری بر پایه‌ی توری دوبعدی گرافن دار

ساره وطنی، حسین طالب، و محمد کاظم مروج فرشی

هسته پژوهشی نانو پلاسمو-فوتونیک، دانشکده مهندسی برق و کامپیوتر، دانشگاه تربیت مدرس، تهران

**چکیده-** برای طراحی یک مدولاتور نوری بازتابی با پهنای نوار باریک و عمق مدولاسیون بالا، برای اولین بار از یک توری دو بعدی گرافن دار در شرایط تزویج بحرانی استفاده کرده‌ایم. نتایج شبیه‌سازی نشان می‌دهد که ساختار پیشنهادی امکان دستیابی به عمق مدولاسیون بیش از ۸۰٪ با پهنای ۷۰ پیکومتری را فراهم می‌آورد. همچنین تاثیر خطاهای احتمالی ساخت در اندازه‌ی دوره‌ی تناوب ( $\Lambda$ ) و ابعاد دندان‌های توری بر طول موج تشدید را بررسی کرده‌ایم. نتایج شبیه‌سازی نشان می‌دهد، تغییر ۱ نانومتری در  $\Lambda$  طول موج تشدید را به اندازه‌ی ۱/۲ نانومتر جابه‌جا می‌کند. در حالی که، اثر همین تغییر در ابعاد دندان‌های توری بر طول موج تشدید بسیار کمتر است. نتایج این تحقیق مسیر دستیابی به مدولاتورهای نوری با عمق مدولاسیون بالا برای استفاده در طول موج‌های مخابرات نوری را هموار می‌کند.

**کلید واژه-** مدولاتور نوری، گرافن، عمق مدولاسیون، تلفات الحاقی

## Optical modulation based on a graphene-loaded 2D grating

Sare Vatani, Hussein Taleb, Mohammad Kazem Moravvej-Farshi\*

Nano Plasmo-Photonic Research Group, Faculty of Electrical and Computer Engineering, Tarbiat Modares University, Tehran, Iran

[sare.vatani@modares.ac.ir](mailto:sare.vatani@modares.ac.ir); [h.taleb@modares.ac.ir](mailto:h.taleb@modares.ac.ir); \*[moravvej@modares.ac.ir](mailto:moravvej@modares.ac.ir)

**Abstract-** To design a narrow-band reflective optical modulator with large modulation depth, we have used a graphene-loaded 2D grating in the critical coupling condition, for the first time. The simulation results show that the designed structure can achieve a modulation depth of more than 80% over a ~70 pm bandwidth. Moreover, to study the effects of the possible fabrication errors on the resonant wavelength, we have investigated the effects of minute changes in the grating period ( $\Lambda$ ) and its teeth dimensions. The results show that a 1-nm error in the  $\Lambda$  results in an about 1.2 shift in the resonant wavelength. Whereas, the effects of the same errors in the grating teeth dimensions are much less significant. These results can pave the way for obtaining narrow bandwidth optical modulators with high modulation depth for optical communication applications.

**Keywords:** Optical Modulator, Graphene, Modulation Depth, Insertion Loss

## 1. Introduction

A high-speed compact optical modulator serves as a fundamental element for optical communication systems. Depending on how an optical modulator modulates the light signal, it can be classified as amplitude, phase, or polarization modulator. Depending on its operation principle, an optical modulator is categorized as all optical, electro-optical, or thermo-optical. Moreover, an optical modulator can be either reflective or absorptive, depending on the type of light-matter interaction responsible for the modulation [1].

Reflective optical modulators, due to their potential application in high-capacity dense wavelength division multiplexing (DWDM) systems, have attracted much attention. They can be replaced for lasers used at the subscriber-end in most bidirectional optical communication systems. A narrow bandwidth optical modulator can be made more environmentally robust and reliable than the expensive narrow-linewidth lasers [2].

A layer of pristine graphene, with unique electrical and optical properties [3, 4], exhibits a constant optical absorption,  $\alpha = e^2/\hbar c$  [5], in which  $\hbar$  is the reduced Planck constant,  $e$  is the elementary electric charge, and  $c$  is the free space light velocity. Moreover, the carrier concentration and optical surface conductivity of graphene can be modulated via modulation of its chemical potential ( $\mu_c$ ), through an appropriate electrical gating scheme [6], making it a prominent candidate to be employed in optical applications [7]. Nonetheless, the limited optical absorption of a 0.34-nm thick monolayer of graphene can be enhanced, by integrating it with dielectric resonators, enhancing the light-matter interaction required for the critical coupling condition [8].

In this paper, taking advantage of a graphene-loaded 2D grating, in the critical coupling condition, we

have designed a narrow-band high-modulation-depth reflective optical modulator.

## 2. Modulator Structure and Operation

Figure 1 illustrates the physical structure of the proposed optical modulator, schematically. It consists of a distributed Bragg reflector (DBR) formed by a stack of  $\text{Si}_3\text{N}_4/\text{SiO}_2$  pairs devised on a Sapphire substrate. In Fig. 1(b),  $h_a$  and  $h_b$  representing the thicknesses of  $\text{SiO}_2$  and  $\text{Si}_3\text{N}_4$  slabs, respectively, each equals a quarter of the wavelength in the respective material. The top  $\text{SiO}_2$  slab in the DBR is sandwiched between two single layers of graphene. On the top of the upper graphene layer, a 2D grating of pitch  $\Lambda$  is formed by a 2D array of Si rods with square cross-sectional areas. Each unit cell of the grating with the underlying forms a resonator at the wavelength  $\lambda = 1550$  nm.

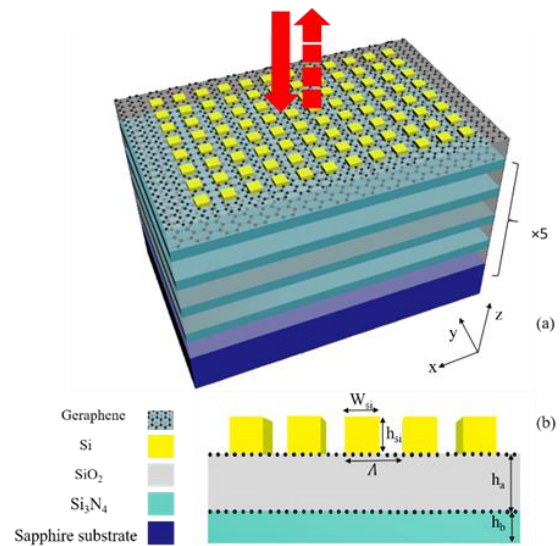


Fig. 1: (a) Schematic of the proposed modulator, (b) side-view of the grating structure.

One can modulate the optical properties of the proposed structure, specifically its reflectance; taking advantage of the tuneable property of the graphene chemical potential ( $\mu_c$ ), and hence its optical conductivity via an appropriate electrostatic gating scheme. The graphene sheet optical conductivity ( $\sigma_s$ ), is related to its chemical potential via the well-known Kubo formula [9]. Moreover,

we can estimate the relative effective permittivity of a graphene layer sandwiched between two dielectric slabs by  $\varepsilon \approx \varepsilon_{av} + i\sigma_s/\varepsilon_0\omega\Delta$ , where  $\varepsilon_{av}$  is the average effective permittivity of the top and bottom slabs,  $\varepsilon_0$  is the free space permittivity, and  $\Delta$  is the thickness of the graphene layer. Hence, the effective relative permittivity of the proposed structure is also tuneable. This property lets us modulate the structure reflectance minima and maxima, as desired for the reflective optical modulators.

Consider a transverse electric (TE) polarized plane wave of center  $\lambda_0=1550$  nm, incident upon the structure top surface, in the  $-z$ -direction. The periodic elements of an appropriately designed structure can provide necessary phase matching between the incident light and subwavelength structures inherent mode, leading to a near-critical coupling condition required for the emergence of a Guided-mode resonance with near-zero reflectance. For this purpose, we choose the design parameters to achieve the critical coupling for the lowest possible chemical potential ( $\mu_{C1}$ ), first. In this condition, the reflectance for the designed structure approaches near zero at a specific wavelength—i.e., the OFF state. Then, we seek for an appropriate chemical potential ( $\mu_{C2} > \mu_{C1}$ ), for which the reflectance spectrum exhibits a suitable shift, providing the ON state with the desired modulation depth of greater than 80%. Notice, the modulation depth for the modulators is determined by the ratio of the minimum to the maximum of the reflectivities for  $\mu_{C1}$  ( $R_1$ ) and  $\mu_{C2}$  ( $R_2$ ), — i.e.  $MD(\lambda) = 1 - \min[R_1 \& R_2] / \max[R_1 \& R_2]$  [6].

Another important characteristic parameter for an optical modulator is its insertion loss ( $IL$ ) that equals the optical loss when the light intensity is maximized — i.e.,  $IL(\text{dB}) = 10 \log R_{\max}$  dB [6].

### 3. Results and Discussions

Using the physical parameters and geometrical dimension given in Table I, we have simulated the reflectance spectrum of the proposed structure, in the wavelength range  $1449 \leq \lambda \leq 1553$ , to characterize

the modulator for two values of  $\mu_C = 120$  meV for OFF state and 370 meV for ON state.

Table 1. The geometrical and physical parameters used in the simulations

Symbol	Definition	Size	Units
$h_{Si}$	Grating height	56	nm
$W_{Si}$	Si rods horizontal dimension	842	nm
$\Lambda$	Grating pitch	998	nm
$h_a$	SiO <sub>2</sub> slab thickness	$\lambda/4n_a$	nm
$h_b$	Si <sub>3</sub> O <sub>4</sub> slab thickness	$\lambda/4n_b$	nm
$n_{Si}$	Si refractive index	3.47	—
$n_a$	SiO <sub>2</sub> refractive index	1.45	—
$n_b$	Si <sub>3</sub> O <sub>4</sub> refractive index	2.13	—
$N$	Number of the pairs of SiO <sub>2</sub> /Si <sub>3</sub> N <sub>4</sub> in the DBR	20	—

The dots and solid line in Fig. 2(a) represents the reflectance spectra for  $\mu_{C1}$  and  $\mu_{C2}$ , respectively. The dots-dashes in the same figure represent the  $MD$  spectrum with a narrow bandwidth of less than 1 nm. Fig. 2(b) illustrates the corresponding insertion loss.

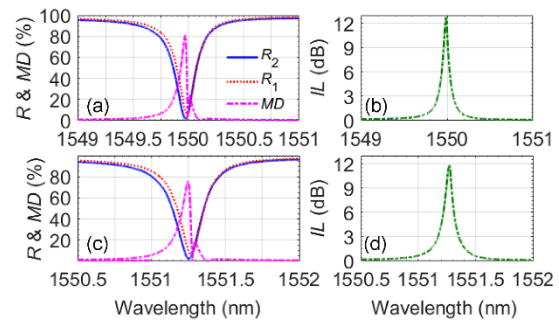


Fig. 2: (a)  $R_1$  (dots),  $R_2$  (solid line), the resulting  $MD$  spectrum (dots-dashes) for  $\Lambda = 998$  nm, and (b) the related  $IL$ ; (c) and correspond to (a) and (b) for  $\Lambda = 999$  nm.

Since the resonance wavelength of the modulator is sensitive to the grating pitch that in turn is affected by the unavoidable fabrication errors, we have repeated the simulations for a 1-nm change in the pitch size (i.e.,  $\Lambda = 999$  nm), keeping the other dimension fixed. Figures 2(c) and (d), illustrate data similar to those of Fig. 2(a) and 2(b), for the new  $\Lambda$ . A comparison of these two sets of data reveals a redshift of  $\Delta\lambda \approx 1.25$  nm in the resonant wavelength.

This wavelength shift is due to the fact that the propagation constant of the guided varies as  $\beta \propto \Lambda^{-1}$  [10]. In other words, as  $\Lambda$  increases, while other grating dimensions are fixed, the effective refractive index and hence the propagation constant of the guided mode decreases, resulting in a redshift in the reflection spectra and hence in the corresponding MD spectrum.

Other grating dimensions ( $h_{Si}$  and  $W_{Si}$ ) are also subject to the fabrication process errors, influencing the modulator characteristics. Figures 3(a) and 3(b) compare the MD and IL spectra for  $h_{Si}=56$  and 60 nm, while other parameters are the same as those in Table I. This comparison shows that a 2-nm increase in the grating teeth height causes a redshift of  $\Delta\lambda \approx 0.7$  nm. This redshift is attributed to an increase of  $\sim 0.47\%$  in the grating aspect ratio ( $h_{Si}/W_{Si}$ ) [11]. Figures 3(c) and 3(d) compare the MD and IL spectra for  $W_{Si}=840$  and 842 nm, while other parameters are the same as those in Table I. This comparison shows that a 2-nm decrease in  $W_{Si}$  causes a redshift of  $\Delta\lambda < 0.1$  nm in the modulator resonant wavelength. In fact, to achieve a 0.7-nm redshift we need to decrease  $W_{Si}$  by  $\sim 56$  nm.

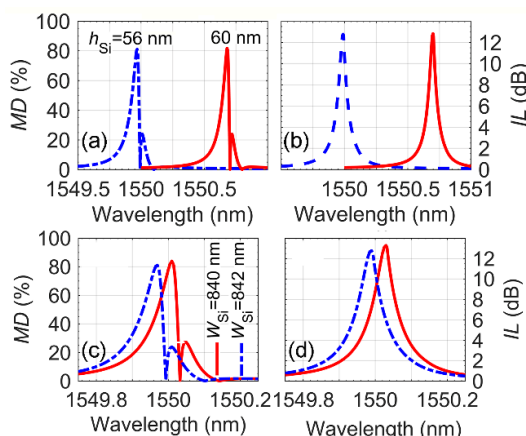


Fig. 3 (a) MD and (b) IL spectra for  $h_{Si}=56$  and 60 nm; (c) and (d) illustrate MD and (b) IL spectra for  $W_{Si}=840$  and 842 nm.

#### 4. Conclusion

We have proposed a multi-layered refractive optical modulator that operates based on the guided-mode resonance of Si grating, devised 20 pairs of  $SiO_2/Si_3N_4$  DBR. The top  $SiO_2$  is sandwiched between two sheets of graphene. By modulating the

graphenes chemical potential between  $\mu_C=120$  meV (OFF state) and 370 meV (ON state), we have achieved a modulation depth of  $\sim 80\%$  insertion of  $\sim 12$  dB over a narrow bandwidth of  $<0.1$  nm, at  $\lambda \sim 1550$  nm. We have also investigated the effects of the grating geometry on the resonant wavelength of the designed modulator.

#### References

- [1] Z. Sun, A. Martinez, and F. Wang, "Optical modulators with 2D layered materials," *Nature Photonics*, vol. 10, no. 4, p. 227, 2016.
- [2] L. Altwegg, A. Azizi, P. Vogel, Y. Wang, and F. Wyler, "LOCNET: A fiber in the loop system with no light source at the subscriber end," *Journal of Lightwave technol.*, vol. 12, no. 3, pp. 535-540, 1994.
- [3] J. Wu, "Ultra-narrow perfect graphene absorber based on critical coupling," *Optics Communications*, vol. 435, pp. 25-29, 2019.
- [4] M. Liu et al., "A graphene-based broadband optical modulator," *Nature*, vol. 474, no. 7349, p. 64, 2011.
- [5] J. R. Piper and S. Fan, "Total absorption in a graphene monolayer in the optical regime by critical coupling with a photonic crystal guided resonance," *ACS Photonics*, vol. 1, no. 4, pp. 347-353, 2014.
- [6] Y. Yao et al., "Electrically tunable metasurface perfect absorbers for ultrathin mid-infrared optical modulators," *Nano Letts.*, vol. 14, no. 11, pp. 6526-6532, 2014.
- [7] S. Yu, X. Wu, Y. Wang, X. Guo, and L. Tong, "2D materials for optical modulation: challenges and opportunities," *Advanced Materials*, vol. 29, no. 14, p. 1606128, 2017.
- [8] C. Guo et al., "Graphene-based perfect absorption structures in the visible to terahertz band and their optoelectronic applications," *Nanomaterials*, vol. 8, no. 12, p. 1033, 2018.
- [9] H. Wang et al., "Transparent Perfect Microwave Absorber Employing Asymmetric Resonance Cavity," *Advanced Science*, 2019.
- [10] S. Peng and G. M. Morris, "Resonant scattering from two-dimensional gratings," *J. Opt. Soc. Am. A*, vol. 13, no. 5, pp. 993-1005, 1996/05/01 1996.
- [11] R. G. Mote, S. F. Yu, W. Zhou, and X. F. Li, "Design and analysis of two-dimensional high-index-contrast grating surface-emitting lasers," *Opt. Express*, vol. 17, no. 1, pp. 260-265, 2009/01/05 2009.